

**Research Article****Histopathological features of non-neoplastic areas of clear cell renal cell carcinoma tissues and clinical outcomes of patients**

Keerakarn Somsuan<sup>1,2</sup>, Ratirat Samon<sup>3</sup>, Yupa Srithongchai<sup>1</sup>, Phattarapon Sonthi<sup>1</sup>, Siripat Aluksanasuwan<sup>2,4</sup> and Natthiya Sakulsak<sup>1\*</sup>

<sup>1</sup> Department of Anatomy, Faculty of Medical Science, Naresuan University, Phitsanulok, 65000

<sup>2</sup> School of Medicine, Mae Fah Luang University, Chiang Rai, 57100

<sup>3</sup> Unit of Pathology, Sawanpracharak Hospital, Nakornsawan, 60000

<sup>4</sup> Cancer and Immunology Research Unit, Mae Fah Luang University, Chiang Rai, 57100

\* Corresponding author: Natthiyak@nu.ac.th

**Naresuan Phayao J.** 2022;15(3): 3-17.

Received: 2 October 2021; Revised: 31 October 2022; Accepted: 27 December 2022

**Abstract**

This study aimed to investigate the histopathological changes in non-neoplastic areas of clear cell renal cell carcinoma tissue, using H&E and PAS staining, and to evaluate the clinical outcomes of patients. Our findings illustrated several aspects of the histopathological features of non-neoplastic areas of renal cancer tissues. It consisted of mononuclear infiltration, adipocyte deposition, interstitial fibrosis with macrophage infiltration, and fibrinoid necrosis of the interlobar arteries. Nodular glomerulosclerosis along with thickening of glomerular basement membranes was abundant in the non-neoplastic area. The hemorrhagic area was remarkable for containing RBC casts and macrophages containing hemosiderin. Additionally, we found necrosis of the renal tubular epithelium, thyroidization, and inflammatory cells casts in the tubular lumen. Most of our patients were elderly and the neoplasms presented mostly in males. The specimens were mostly found to show chronic pyelonephritis (64.71%) and hemorrhagic areas (88.24%). The patients were observed to have metastatic status (17.65%) and had been diagnosed with chronic pyelonephritis. All 8/17 patients had a comorbidity e.g. hypertension (HT), chronic kidney disease (CKD), diabetes mellitus (DM). We noted that ccRCC patients presenting with chronic pyelonephritis and with metastases had cumulative survival rates lower than those patients without chronic pyelonephritis (72% vs. 100%). Hence, evaluation of histopathological changes in non-neoplastic renal parenchyma should be performed for patients with RCC, to improve management and treatment options, that may prevent accelerated function failure of the single remaining kidney, especially in patients with a background of medical diseases, including diabetes or hypertension.

**Keywords:** Non-neoplastic area, Clear cell, Renal cell carcinoma, Histopathological features

## Introduction

Incidence rates of renal cell carcinoma (RCC) have been increasing in the developed countries over the past half-century [1]. In 2020, RCC is the sixth most commonly diagnosed malignancy in men and the 10th in women in the USA, estimated new case rates being 45,520 and 28,230 cases [2]. The main subtype of renal cancer is clear cell renal cell carcinoma (ccRCC), it accounts for 70-80% of diagnoses whereas non-clear cell histologic types represent the remaining 20-30% [3]. Although the detection of small tumors by cross-sectional imaging and subsequent removal with surgery has increased, metastases and mortality rates in patients with RCC have still predominantly increased [4]. The long-term complications of nephrectomy in renal tumor patients are increases of glomerular filtration rate, hypertension, and proteinuria, associated with the development of chronic kidney disease (CKD) [5]. In 2006, Bijol and his colleagues [6] reported that the pathologic changes in non-neoplastic renal parenchyma of renal tumors were the significant parameter to predict the outcome of contralateral kidney function. They found that patients with severe histopathologic features, including severe parenchymal scarring with 20% or more global glomerulosclerosis, showed a significant increase in serum creatinine from the preoperative period to 6 months after surgery, indicative of progressive decline in kidney function. A recent study has reported that pathological findings, that included vascular sclerosis with parenchymal scars (36%) and chronic pyelonephritis (18%), were mostly found at sites of non-neoplastic tissue in patients with ccRCC. Moreover, other features were mesangial hypercellularity (4%), focal segmental glomerulonephritis (8%) and membranoproliferative glomerulonephritis (6%) [7]. The precise examination of non-neoplastic

renal parenchyma was an important evaluation in predicting patients at risk for worsening of CKD progression after nephrectomy [6, 8, 9]. The purpose of this study was to examine and describe the histopathological changes in non-neoplastic areas of clear cell renal cell carcinoma tissues, and to evaluate the associated clinical outcomes of patients.

## Materials and Methods

This study was a retrospective study, approved by the Human Ethic Review Board of Sawan Pracharak hospital, Nakhon Sawan, Thailand in 2017 (No. 47/2560) and by Naresuan University Ethical Committee for Human Research (NU-IRB) (No. 0489/61), COE No. 115/2018. Tissue was collected from the Unit of Pathology, Sawan Pracharak hospital, Nakhon Sawan, Thailand during 2013-2017. Seventeen nephrectomy specimens were immediately fixed in formalin fixation. After tissue processing and embedding, then formalin fixed, paraffin embedded (FFPE) samples of patients diagnosed with clear cell subtype of RCC were produced and collected. There were 6 clear cell RCC, Fuhrman nuclear grade I (ccRCC, G1) and 11 clear cell RCC, Fuhrman nuclear grade II (ccRCC, GII) as identified by the pathologist. The clinical data such as age, sex, and pathological findings i.e. gross and microscopic features were recorded. The gross description and microscopic features of the tumor specimens i.e. laterality, tumor size, hemorrhagic area, chronic pyelonephritis, renal invasion, and lymph node involvement etc., were recorded. The FFPE samples were cut and hematoxylin and eosin staining performed, along with Periodic acid-Schiff (PAS) staining, using the standardized methods. The microscopic features of normal, non-neoplastic, and cancer areas were studied and

photographed under an Olympus BX50 light microscope (Olympus; Tokyo, Japan).

### Statistical analysis

Ethical approval from the ethical committee of the institute was taken and a descriptive analysis of the data was done and described by number of cases and percentage. The quantitative data were presented as mean  $\pm$  SD. The association between chronic pyelonephritis status and metastases was evaluated by Kaplan-Meier analysis and log- rank test. All statistical analyses were done through the SPSS software (version 16.0) (SPSS; Chicago, IL),  $p$ -value  $< 0.05$  was considered statistically significance.

## Results

### The clinical data of patients and gross description of tumor specimens

Seventeen patients with RCC who had undergone renal nephrectomy were enrolled. The patients' age ranged from 50 to 91 years and the mean age of the patients was  $62.06 \pm 10.32$  years. Among the patients, 9 patients (52.94%) were  $\geq 60$  years, and 8 patients (47.06%) were  $< 60$  years. As regards sex, 13 patients (76.47%) were male and 4 patients (23.53%) were female. The RCC detected at the right side was 10 cases (58.82%) and the left side was 7 cases (41.17%). The Fuhrman nuclear grading is the most widely

used grading system for grading renal cell carcinoma, as has been described in previous studies [10, 11]. In this study, there were 6 clear cell RCCs, Fuhrman nuclear grade I (ccRCCs, GI) (35.29%) and 11 clear cell RCCs, Fuhrman nuclear grade II (ccRCCs, GII) (64.71%). Chronic pyelonephritis was detected in 11 patients (64.71%), but not detected in 6 patients (35.29%). Hemorrhagic areas were observed in 15 cases (88.24%); however, the size of hemorrhagic area was varied. Of these patients, 4 cases (25.53%) presented with renal invasion, but was not observed in 13 cases (76.47%). The AJCC stages were categorized by following the American Joint Committee on Cancer (AJCC) tumor- node-metastasis (TNM) staging [12, 13]. There were 6 cases of stage I (35.29%), 3 cases (17.67%) of stage II, 6 cases of stage III (35.29%), and 2 cases (11.76%) of stage IV. Of note, three patients (17.65%) had metastatic status and 10 patients (58.82%) did not. All of these findings are summarized in Table 1. The relevant clinical details of all patients and their comorbidities are reported in the Table 2. Patients presenting with the metastases, in the lung (1 case) and brain (2 cases), were also diagnosed with chronic pyelonephritis. A total of 8 cases had comorbidities e.g. hypertension (HT), chronic kidney disease (CKD), liver disease, gall stones, hyperlipidemia, cystic kidney disease, DM type II, cardiovascular disease, and lung disease.

**Table I** Clinical data of ccRCC patients and gross description of tumor specimens (N = 17)

Clinical data and gross description	No. of patient (%)
<b>Age (years)</b>	
≥ 60 years	9 (52.94%)
< 60 years	8 (47.06%)
<b>Sex</b>	
Male	13 (76.47%)
Female	4 (23.53%)
<b>Laterality</b>	
Right	10 (58.82%)
Left	7 (41.17%)
<b>Fuhrman nuclear grading</b>	
ccRCC (grade I)	6 (35.29%)
ccRCC (grade II)	11 (64.71%)
<b>Chronic pyelonephritis status</b>	
Present	11 (64.71%)
No	6 (35.29%)
<b>Hemorrhage</b>	
Present	15 (88.24%)
No	2 (11.74%)
<b>Renal invasion</b>	
Present	4 (25.53%)
No	13 (76.47%)
<b>AJCC stages</b>	
Stage I	6 (35.29%)
Stage II	3 (17.67%)
Stage III	6 (35.29%)
Stage IV	2 (11.76%)
<b>Metastases</b>	
Present	3 (17.65%)
No	10 (58.82%)

**Table II** Clinical data and comorbidity of ccRCC patients

No	Age (years)	Sex	Laterality	Pathological grading	Hemorrhage	Chronic pyelonephritis	AJCC stage	Metastatic recurrence (I-IV)	Comorbidity
1	59	Male	Right	ccRCC (G1)	No	Present	3	No	No
2	76	Male	Right	ccRCC (G1)	No	No	3	No	No
3	53	Male	Right	ccRCC (G1)	Present	Present	1	No	Mild fatty liver, Gall stone, Acute cholecystitis
4	91	Male	Right	ccRCC (G1)	Present	No	1	No	No
5	50	Male	Right	ccRCC (G1)	Present	Present	1	No	No
6	56	Female	Left	ccRCC (G1)	Present	No	1	No	HT
7	69	Female	Right	ccRCC (G2)	Present	Present	1	No	No
8	64	Male	Right	ccRCC (G2)	Present	No	2	No	HT, Hyperlipidemia, Cystic kidney disease
9	56	Female	Left	ccRCC (G2)	Present	No	3	No	No
10	61	Male	Left	ccRCC (G2)	Present	No	4	No	Gall stone,
11	51	Male	Left	ccRCC (G2)	Present	Present	4	No	Arteriosclerosis of aorta
12	65	Male	Right	ccRCC (G2)	Present	Present	3	No	No
13	64	Male	Left	ccRCC (G2)	Present	Present	3	No	DM type II, HT Pneumonia,
14	67	Male	Right	ccRCC (G2)	Present	Present	3	Yes (lung)	Adrenal insufficiency
15	52	Male	Left	ccRCC (G2)	Present	Present	2	Yes (brain)	HT, CKD at LK, RCC & stone at RK
16	65	Male	Right	ccRCC (G2)	Present	Present	1	Yes (brain)	DM type II, HT, Liver cirrhosis
17	56	Female	Left	ccRCC (G2)	Present	Present	2	No	HT, Inflammatory liver disease, Mild fatty liver

HT, hypertension; CKD, chronic kidney disease; LK, left kidney; RK, right kidney.

### Histopathological features of non-neoplastic areas of ccRCC tissues

The microscopic structures of normal, non-neoplastic, and cancer areas were observed and illustrated in the Figure 1. The normal areas showed remarkable normal structures of the capsule, cortex, and medulla regions of the kidney (Figure 1A-C).

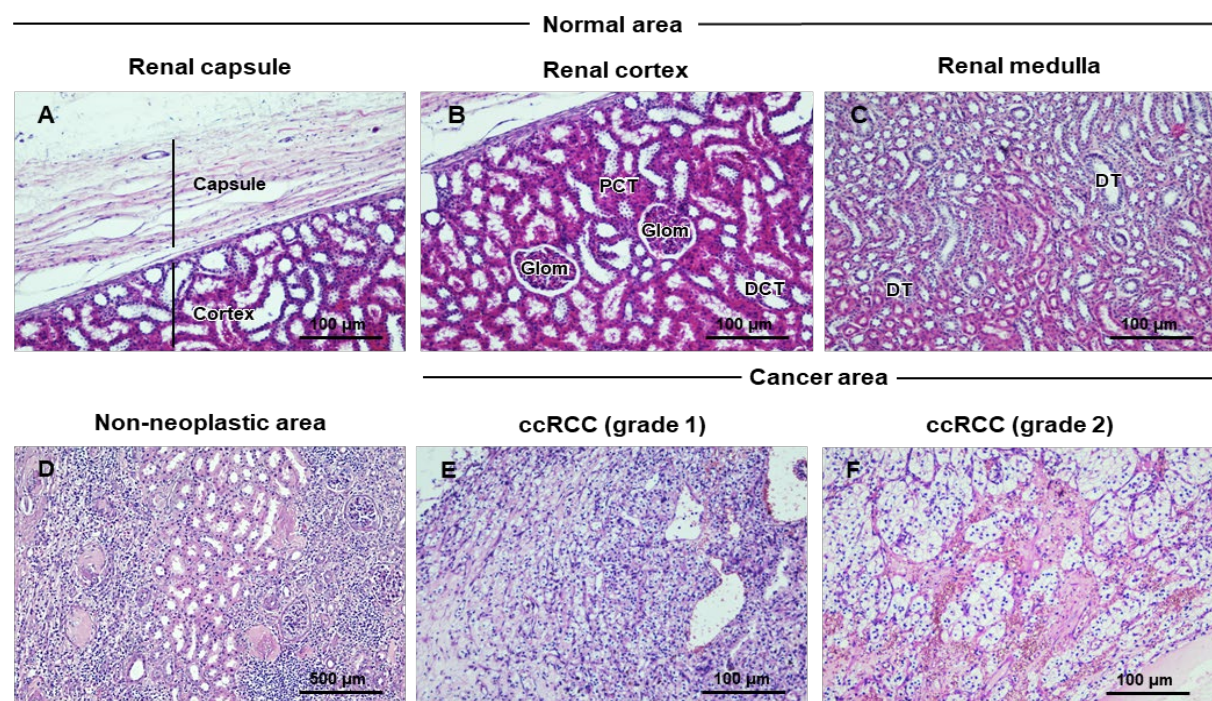


**Figure 1** Histological features of normal, non-neoplastic, and cancer areas of nephrectomy specimens of patients with ccRCC.

(A-C) Normal kidney tissue consists of capsule (A), cortex (B), and medulla (C). The histological structures of glomerulus (glom), proximal (PCT), and distal convoluted tubules (DCT) are demonstrated. (D) Non-neoplastic area, which is an area surrounding cancer area, is shown. (E-F) RCC tissues, including ccRCC (grade 1) (E) and ccRCC (grade 2) (F) are demonstrated. The neoplastic cells are shown abundant clear cytoplasm in ccRCC (grade 2) tissues in the Figure 1F. All images are represented at 100x and 200x magnifications, scale bars are 500 and 100  $\mu$ m, respectively.

Non-neoplastic areas revealed several microscopic changes (Figure 1D). The cancer areas illustrated the characteristics of cancerous clear cells that were confirmed by the Fuhrman nuclear grading of ccRCC (Figure 1E-F). We focused on the histopathological features of the non-neoplastic areas of ccRCC tissue to include the altered features. At the cortex of non-neoplastic areas, mononuclear infiltration was mostly found, presenting with adipocyte deposition (Figure 2A-B). In the non-neoplastic parenchyma, interstitial fibrosis was abundant with aggregation of mononuclear cells and macrophage infiltration (Figure 2C-D). The interlobular artery showed circumferential fibrinoid necrosis with associated leukocyte infiltration (Figure 2E-F).

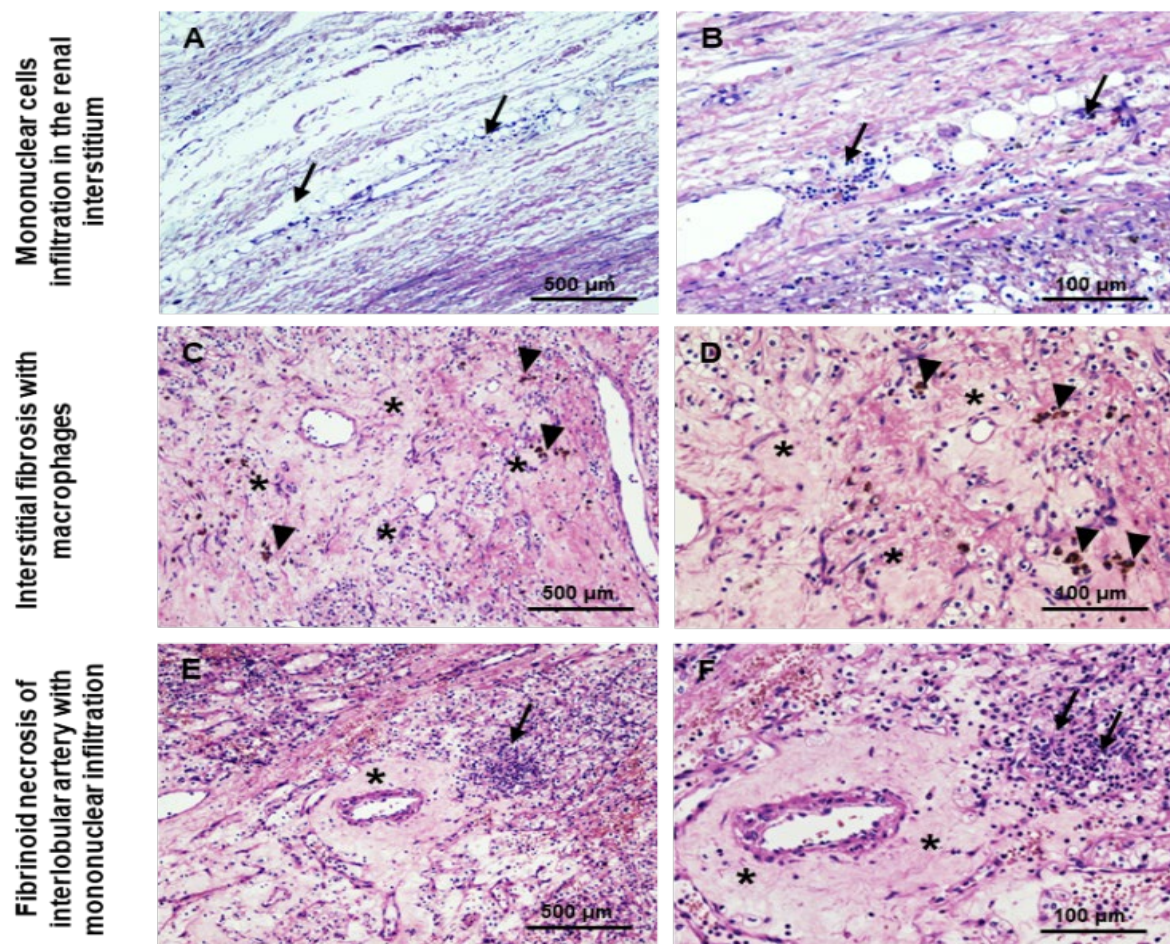


**Figure 2** Histological changes in non-neoplastic area of patients with ccRCC: Mononuclear cells infiltration and interstitial fibrosis.

The histological structures of (A-B) mononuclear cells infiltration (arrow) in the renal interstitium, (C-D) The interstitial fibrosis (asterisk) with macrophages infiltration (head arrow) presents in renal parenchyma of non-neoplastic area, and (E-F) fibrinoid necrosis of interlobular artery (asterisk) with mononuclear cells infiltration (arrow) are demonstrated. All images are represented at 100x and 200x magnifications, scale bars are 500 and 100  $\mu\text{m}$ , respectively.

In addition, the hemorrhagic areas were remarkable, showing interstitial red blood cell (RBC) extravasation, RBC casts and interstitial hemorrhage (Figure 3A-B). Several macrophages contained strong amounts of brown pigment consistent with iron (hemosiderin deposits) (Figure 3C-D). Histological changes of the glomeruli were

predominantly found in the non-neoplastic areas. It revealed glomerulosclerosis and thickening of the glomerular basement membranes (GBMs), as well as dilation of Bowman's capsule (Figure 4A-B), fibrosis and thickening of Bowman's capsule (Figure 4C-D), and nodular glomerulosclerosis presenting with arteriosclerosis (Figure 4E-F).

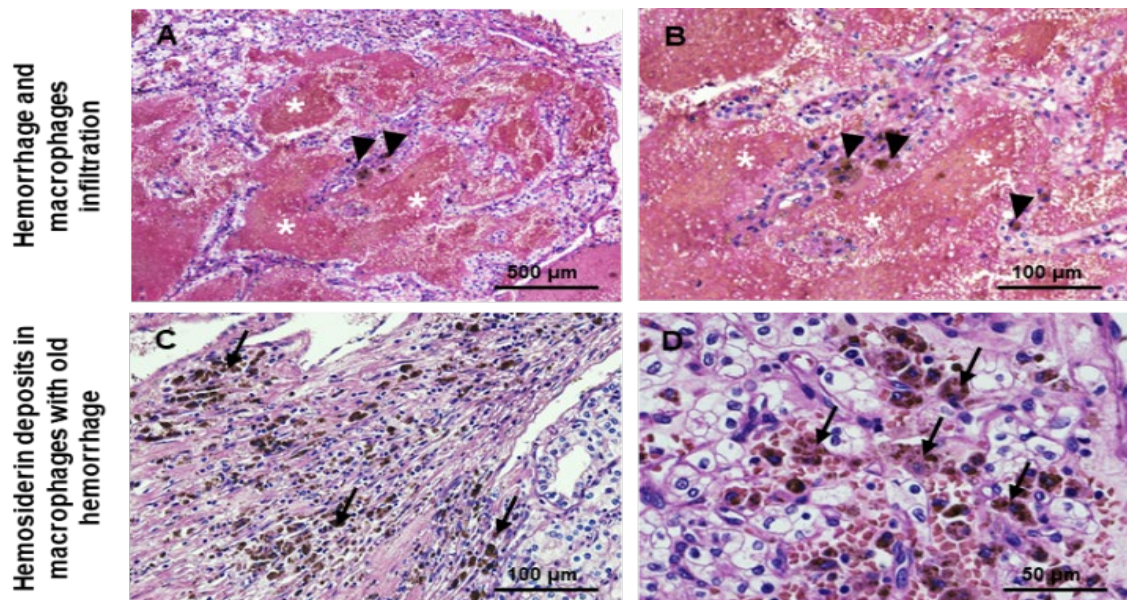


**Figure 3** Histological changes in non-neoplastic area of patients with ccRCC: Hemorrhage, macrophages infiltration containing hemosiderin.

The histological structures of (A-B) hemorrhage (white asterisk) and macrophages infiltration (head arrow) are shown. (C-D) Hemosiderin (black arrow) in tumor associated macrophages presents in old hemorrhagic area. All images are represented at 100x, 200x, and 400x magnifications, scale bars are 500, 100, and 50  $\mu\text{m}$ , respectively.

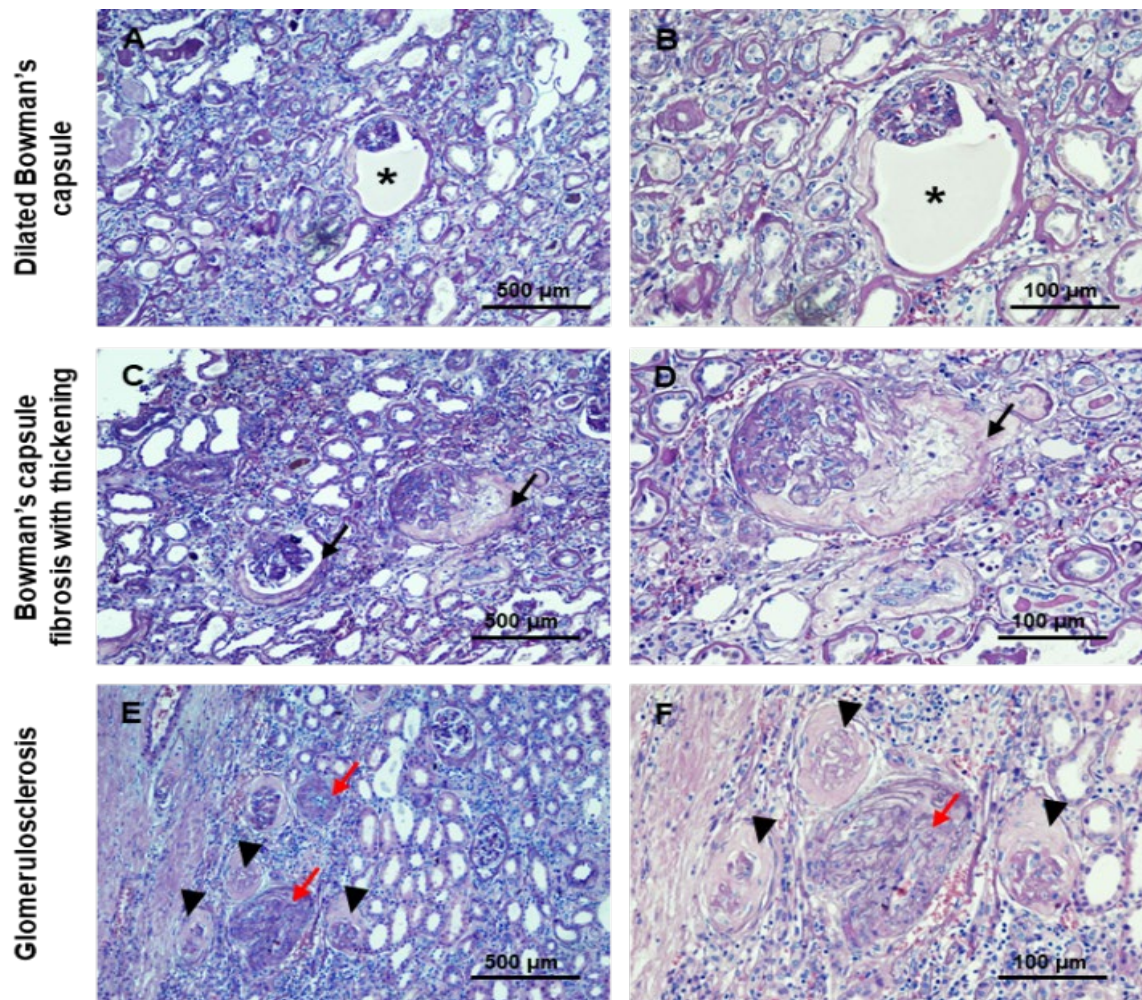


**Figure 4** Histological changes in non-neoplastic area of patients with ccRCC: Abnormalities of the glomeruli.

The aberrancies of glomeruli in non-neoplastic area of ccRCC tissues include (A-B) the dilation of Bowman's capsule (asterisk), (C-D) the fibrosis and thickening of Bowman's capsule (black arrow), and (E-F) the glomerulosclerosis (head arrow) and arteriosclerosis (red arrow). All images are represented at 100x and 200x magnifications, scale bars are 500 and 100  $\mu\text{m}$ , respectively.

The non- neoplastic tissues showed abundant necrosis of the renal tubular epithelium, that was lined with distinctive large eosinophilic cells (Figure 5A-B), thyroidization, with atrophic tubules filled with eosinophilic, colloid- appearing casts (Figure 5C-D), inflammatory cells casts in the tubular lumen ( Figure 5E- F) and intratubular

hemorrhage ( Figure 5G- H). PAS staining was performed to confirm the thickening of GBMs, Bowman's capsule, and basement membranes of the renal tubules as well as arteriosclerosis, that was represented as strong magenta staining (Figure 6A-F). Interstitial fibrosis appeared brightly eosinophilic and smudged (Figure 6G-H).

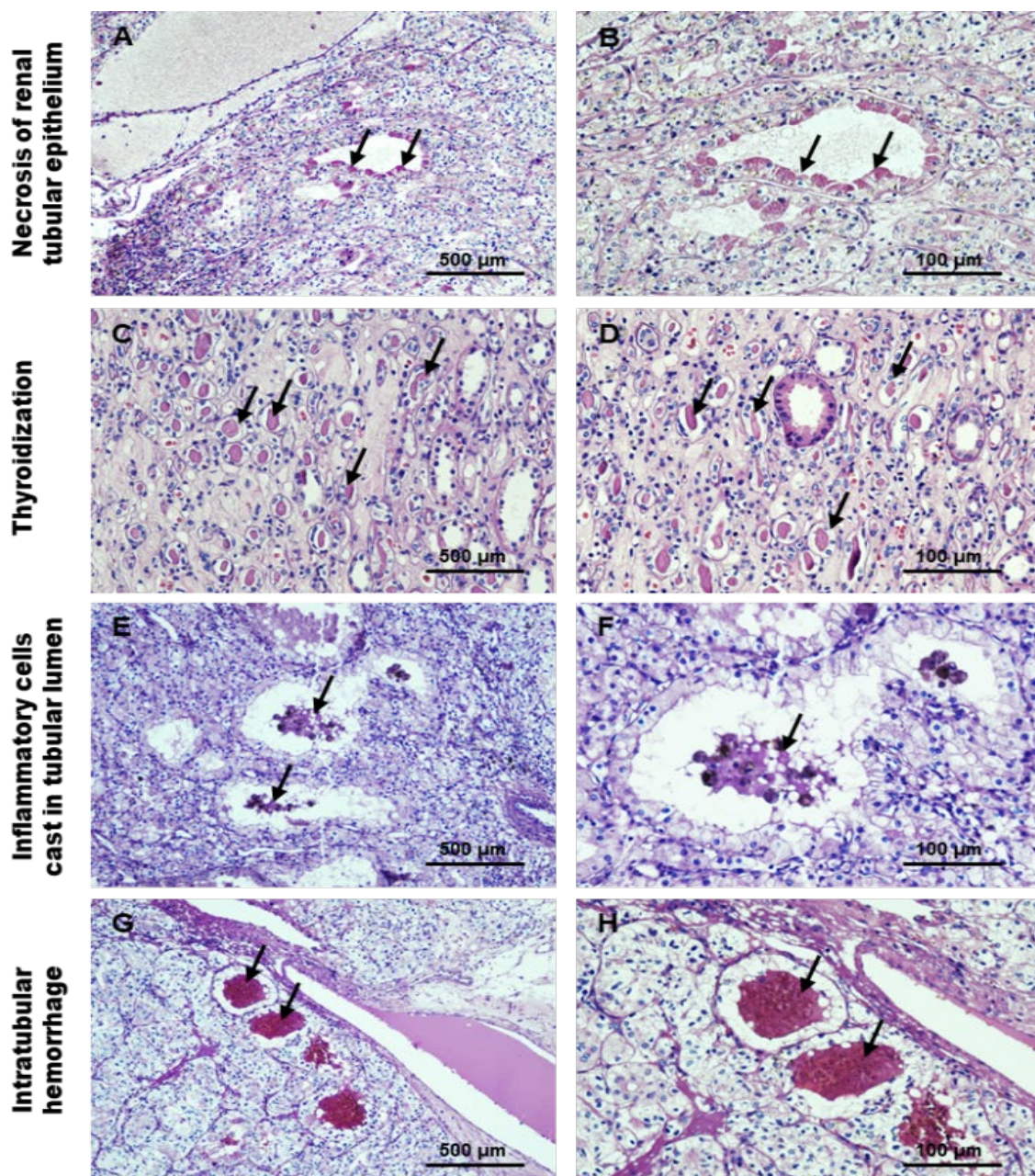


**Figure 5** Histological changes in non-neoplastic area of patients with ccRCC: Abnormalities of the renal tubules.

The abnormal appearances of renal tubules in non-neoplastic area of ccRCC tissues include (A-B) necrosis of renal tubular epithelium, (C-D) thyroidization, (E-F) inflammatory cells cast in tubular lumen, and (G-H) intratubular hemorrhage. All images are represented at 100x and 200x magnifications, scale bars are 500 and 100  $\mu\text{m}$ , respectively.

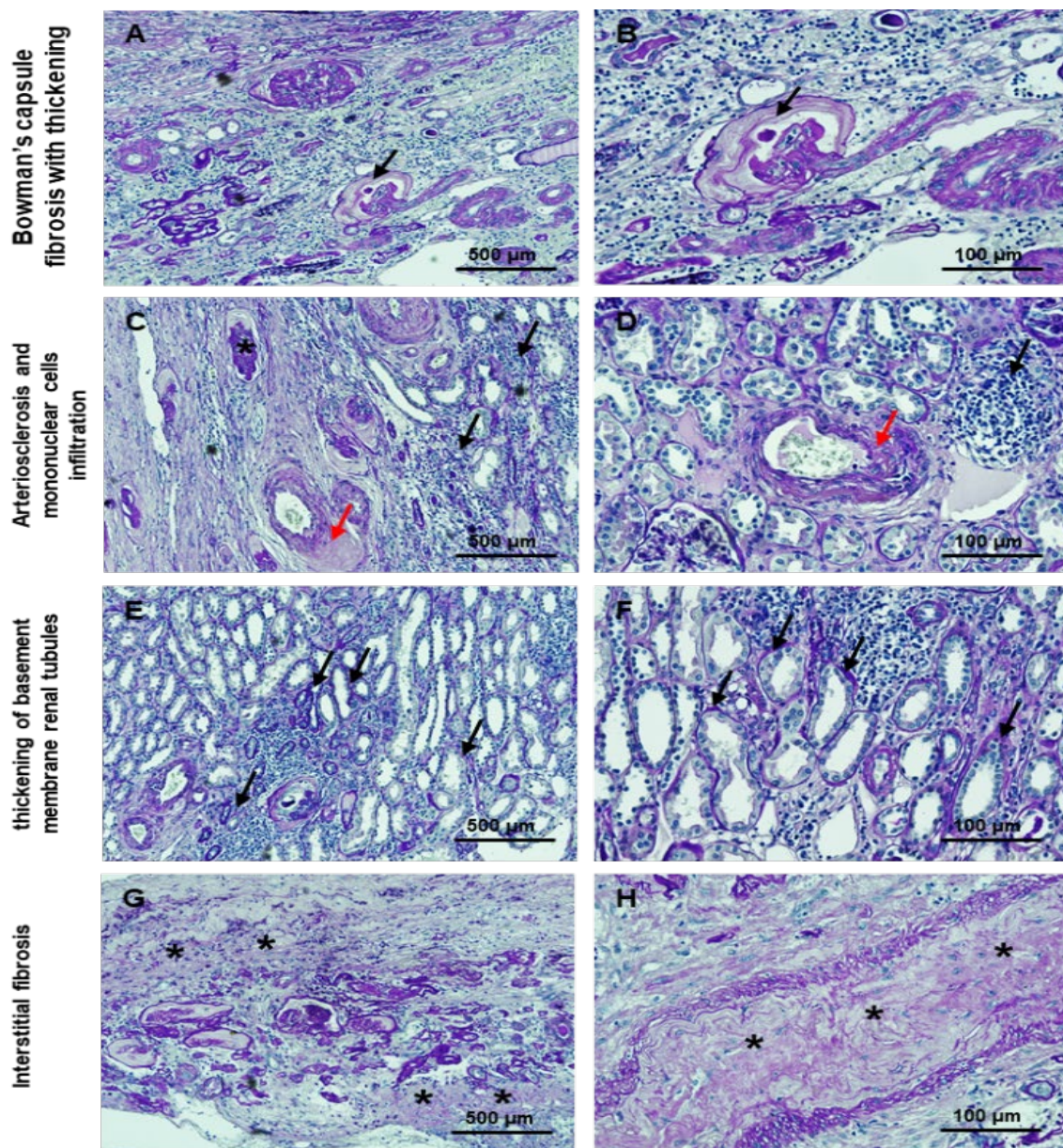


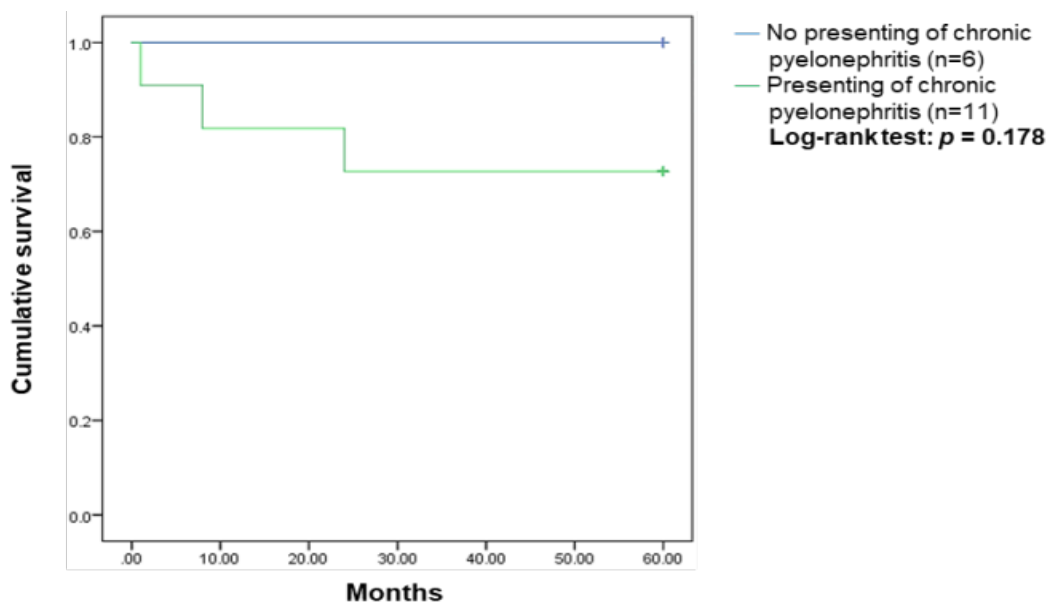
**Figure 6** Histological changes in non-neoplastic area of patients with ccRCC: Abnormalities of the glomeruli and the renal tubules using the PAS staining.

The abnormal appearances of glomeruli and renal tubules in non-neoplastic area of ccRCC tissues were confirmed using PAS staining. (A-B) fibrosis and thickening of Bowman's capsule, (C-D) arteriosclerosis (red arrow) and mononuclear cells infiltration (black arrow), (E-F) the thickening of basement membrane of renal tubules (black arrow) with mononuclear cell infiltration are shown. (G-H) The interstitial fibrosis in non-neoplastic area is indicated as the black asterisk. All images are represented at 100x and 200x magnifications, scale bars are 500 and 100  $\mu\text{m}$ , respectively.

### Prognosis of ccRCC patients presenting of chronic pyelonephritis and metastases

Finally, the prognosis of ccRCC patients presenting of chronic pyelonephritis and metastases was analyzed. RCC patients with non-presentation of chronic pyelonephritis and no

metastatic events (n=6/6) had a cumulative survival of 100%. Log-rank test revealed a tendency of metastatic development in patients with chronic pyelonephritis (n= 3/11) and cumulative survival was 72.2%; however, the *p*-value did not reach a statistically significant level (Figure 7).



Case Processing Summary				
0 no, 1 chronic	Total N	N of Events	Censored	
			N	Percent
no chronic	6	0	6	100.0%
chronic	11	3	8	72.7%
Overall	17	3	14	82.4%

**Figure 7** Kaplan-Meier curve shows the cumulative survival in RCC patients compared between presenting (n = 11) and non-presenting of chronic pyelonephritis (n = 6).

The cumulative survival of RCC patients presenting of chronic pyelonephritis (green line) had a tendency of shorter than those with RCC patients without chronic pyelonephritis (blue line). Log-Rank test was no significant difference between groups (*p* = 0.178, N = 17).

## Discussion and Conclusion

Cigarette smoking, diabetes mellitus, hypertension, obesity, physical inactivity, and increasing age, are well-established risk factors for RCC. Impaired kidney function is independently associated with these diseases [14]. Radical or partial nephrectomy is still the standard treatment of renal neoplasms. The development of chronic kidney disease (CKD), associated with radical nephrectomy [15]. The underlying mechanisms of the development of CKD after nephrectomy have been previously explained by the structural and functional alterations of the remaining nephrons. Maladaptive appearances of CKD were glomerulosclerosis, vascular sclerosis and tubulointerstitial fibrosis [16]. Notably, several studies have confirmed that the relevant evaluation of the histopathological changes of non-neoplastic pathology in tumor nephrectomy specimens is necessary for early detection and for provision of preventive and clinical treatment modalities [6, 8, 17-19].

Our findings illustrated the important histopathologic features that are found in non-neoplastic areas of clear cell renal cell carcinoma tissues and the related clinical outcomes of the patients. Most of our patients were of similar same age and the neoplasms mostly present in male subjects. The specimens confirmed chronic pyelonephritis (64.71%) and hemorrhagic areas (88.24%) of cases. Patients with confirmed metastatic status comprised (17.65%) and they were also diagnosed with chronic pyelonephritis.

All 8/17 patients had at least one comorbidity e.g. hypertension (HT), chronic kidney disease (CKD), Diabetes mellitus (DM). The histopathological abnormalities of the non-neoplastic areas included mononuclear infiltration, adipocyte deposition, interstitial fibrosis with

macrophage infiltration, and fibrinoid necrosis of interlobar arteries (Figure 2). Furthermore, the hemorrhagic area was remarkable for the presence of RBC casts, and the associated macrophages contained hemosiderin (Figure 3). Nodular glomerulosclerosis along with thickening of glomerular basement membranes (GBMs), dilation of Bowman's capsule, fibrosis and thickening of Bowman's capsule were abundant in the non-neoplastic areas (Figure 4). Additionally, necrosis of renal tubular epithelium, thyroidization, and inflammatory cells casts in the tubular lumen (Figure 5) was noted. PAS staining has been suggested for use in the evaluation of non-neoplastic renal parenchymal sections by the College of American Pathologists checklist protocol [20]. Thus, we also stained, using PAS staining, to confirm the histological changes in our study.

Our result was consistent with a previous study, they reported that 10% patients had unremarkable parenchyma [6]. The glomerular filtration rate could be predicted by the severity of glomerulosclerosis. A decrease in glomerular filtration rate by 9% from baseline would be predicted for each 10% increase in glomerulosclerosis [21]. In 2013, Salvatore and colleagues [17] have reported that the proportion of vascular sclerosis, glomerulosclerosis, and interstitial fibrosis and tubular atrophy were prescriptive parameters for the increase of creatinine levels following nephrectomy. Our results demonstrated that ccRCC patients presenting with chronic pyelonephritis and metastatic events had a cumulative survival of 72%. However, the association of chronic pyelonephritis status and the cumulative survival has not been previously reported, so we can highlight the importance of chronic pyelonephritis status in patients with ccRCC.

In conclusion, progressive staging and rate of metastases of renal cancer were higher in patients after renal nephrectomy, where the histology confirmed chronic pyelonephritis. Also the increased rates of renal failure in the remaining kidney may be because of the structural and functional alterations of the remaining nephrons after nephronal loss. This could also be associated with age- related changes and the presence of comorbidities. Therefore, evaluation of histopathological changes in non- neoplastic renal parenchyma should be provided early for patients with RCC to improve management and treatment options that may prevent accelerated function failure of the single remaining kidney, especially in patients with a background of medical diseases including diabetes or hypertension.

### Acknowledgements

This study was supported by the National Science, Research and Innovation Fund (NSRF); grant number R2564B002 and Faculty of Medical Science, Naresuan University, Phitsanulok, Thailand. The authors thank Dr. Roger Timothy Callaghan, MD. for his assistance with preparing the English language.

### References

1. Padala SA, Barsouk A, Thandra KC, Saginala K, Mohammed A, Vakiti A, et al. Epidemiology of Renal Cell Carcinoma. *World J Oncol* 2020;11(3):79-87.
2. Siegel RL, Miller KD, Jemal A. Cancer statistics, 2020. *CA: Cancer J Clin* 2020;70(1):7-30.
3. Rini BI, Campbell SC, Escudier B. Renal cell carcinoma. *Lancet* 2009;373(9669):1119-32.
4. Capitanio U, Montorsi F. Renal cancer. *Lancet* 2016;387(10021):894-906.
5. Ellis RJ. Chronic kidney disease after nephrectomy: a clinically- significant entity? *Transl Androl Urol* 2019;8(Suppl 2):S166-S74.
6. Bijol V, Mendez GP, Hurwitz S, Rennke HG, Nosé V. Evaluation of the nonneoplastic pathology in tumor nephrectomy specimens: predicting the risk of progressive renal failure. *Am J Surg Pathol* 2006;30(5):575-84.
7. Noroozinia F, Makhdoomi K, Behnamfard H, Mohammadi S, Dindarian S, Bagheri M, et al. The pathological evaluation of nonneoplastic kidney disorder in tumor nephrectomy specimens. *Saudi J Kidney Dis Transpl* 2018;29(3):586-90.

8. Henriksen KJ, Meehan SM, Chang A. Non-neoplastic renal diseases are often unrecognized in adult tumor nephrectomy specimens: a review of 246 cases. *Am J Surg Pathol* 2007;31(11):1703-8.
9. Bonsib SM, Pei Y. The Non-neoplastic Kidney in Tumor Nephrectomy Specimens: What Can it Show and What is Important? *Adv Anat Pathol* 2010;17(4):235-50.
10. Corti B, Zucchini N, Fabbrizio B, Martorana G, Schiavina R, Grigioni ADE, et al. Pathology and Molecular Pathogenesis of Renal Cell Carcinoma. *Eur Urol Suppl* 2006;5(8):573-9.
11. Fuhrman SA, Lasky LC, Limas C. Prognostic significance of morphologic parameters in renal cell carcinoma. *Am J Surg Pathol* 1982;6(7):655-63.
12. Petejova N, Martinek A. Renal cell carcinoma: Review of etiology, pathophysiology and risk factors. *Biomed. Pap. Med. Fac. Univ. Palacky Olomouc Czech Repub* 2016;160(2):183-94.
13. Edge SB, Compton CC. The American Joint Committee on Cancer: the 7th Edition of the AJCC Cancer Staging Manual and the Future of TNM. *Ann Surg Oncol* 2010;17(6):1471-4.
14. Chow W- H, Dong LM, Devesa SS. Epidemiology and risk factors for kidney cancer. *Nat Rev Urol* 2010;7(5):245-57.
15. Streja E, Kalantar- Zadeh K, Molnar MZ, Landman J, Arah OA, Kovesdy CP. Radical versus partial nephrectomy, chronic kidney disease progression and mortality in US veterans. *Nephrol Dial Transplant* 2016;33(1):95-101.
16. Bijol V, Batal I. Non- neoplastic Pathology in Tumor Nephrectomy Specimens. *Surg Pathol Clin* 2014;7(3):291-305.
17. Salvatore SP, Cha EK, Rosoff JS, Seshan SV. Nonneoplastic renal cortical scarring at tumor nephrectomy predicts decline in kidney function. *Arch Pathol Lab Med* 2013;137(4):531-40.
18. Garcia- Roig M, Gorin MA, Parra- Herran C, Garcia- Buitrago M, Kava BR, Jorda M, et al. Pathologic evaluation of non- neoplastic renal parenchyma in partial nephrectomy specimens. *World J Urol* 2013;31(4):835-9.
19. Truong LD, Shen SS, Park MH, Krishnan B. Diagnosing nonneoplastic lesions in nephrectomy specimens. *Arch Pathol Lab Med* 2009;133(2):189-200.
20. Higgins JP, McKenney JK, Brooks JD, Argani P, Epstein JI. Recommendations for the reporting of surgically resected specimens of renal cell carcinoma: the Association of Directors of Anatomic and Surgical Pathology. *Hum Pathol* 2009;40(4):456-63.
21. Gautam G, Lifshitz D, Shikanov S, Moore JM, Eggner SE, Shalhav AL, et al. Histopathological predictors of renal function decrease after laparoscopic radical nephrectomy. *J Urol* 2010;184(5):1872-6.